Proceedings of the ASME 2015 Pressure Vessels and Piping Conference
PVP2015
July 19-23, 2015, Boston, Massachusetts, USA

PVP2015-45820

CRACK TIP STRAIN DISTRIBUTIONS AND THEIR IMPLICATIONS TO CRACK GROWTH RATE DUE TO STRESS CORROSION CRACKING

Shin-Jang Sung, Nikhil Kotasthane, Yugo Ashida
and Jwo Pan
Mechanical Engineering
University of Michigan
Ann Arbor, MI 48109, USA

ABSTRACT

In this paper, stress and strain distributions near a crack tip in a round compact tension specimen of elastic-plastic materials are obtained by finite element analyses. The strain distributions are used to explore the use of the crack tip strain distributions for crack growth rate models due to stress corrosion cracking in unirradiated and irradiated steels with different yield stresses and hardening behaviors. Both power-law hardening and perfectly plastic materials are considered. The computational results indicate that the critical radial distance to the tip based on the crack tip opening displacement is outside of the Hutchinson-Rice-Rosengren (HRR) dominant zone for power-law hardening materials in a round compact tension specimen under the stress intensity factor typically considered for stress corrosion cracking. For both the power-law hardening and perfectly plastic materials, the computational results show that the strain distributions are different from those of the analytical solutions for the range of the radial distance larger than the critical radial distance based on the crack opening displacement within the plastic zones. The computational results suggest that for the stress intensity factor typically considered for stress corrosion crack growth rate models, computational results are needed to estimate the strain rate for developing crack growth rate models to correlate to the experimental data.

INTRODUCTION

Andresen and Ford [1] developed a well-accepted, semi-empirical model based on the oxide film rupture-slip dissolution mechanism to predict crack growth rate (CGR) in a boiling water reactor (BWR) system. Passivity from oxide growth renders structural materials usable in high temperature water and its disruption by plastic strain is the origin of the material and water chemistry effects on environmentally assisted cracking. By applying Faraday's law and considering the competition between oxide film formation and oxide rupture at the crack tip, they expressed the crack growth rate (da/dt) as

$$\frac{da}{dt} = \frac{M}{z \cdot \rho \cdot F} \cdot \frac{i_0}{1-m} \cdot \left(\frac{t_0}{\varepsilon_f} \right)^m \cdot \left(\dot{\varepsilon}_{ct} \right)^m \tag{1}$$

where M and ρ are the atomic weight and the density of metal, respectively, z is the change in charge due to oxidation, F is Faraday's constant, i_0 is the electrochemical current density of the new surface before the formation of an oxide film, m is the exponent of current decay curve (showing the characteristic of oxide film formation), t_0 is the time period of oxide film formation, ε_f is the fracture strain of oxide film, and $\dot{\varepsilon}_{ct}$ (or $d\varepsilon_{ct}/dt$) is the strain rate at a characteristic distance r_0 ahead of the crack tip. The strain rate ahead of the crack tip plays a key role in the crack growth rate. However, it is difficult to precisely determine its value, and the location at which it should be evaluated. Shoji et al. [2] expressed the crack tip strain rate in terms of the strain gradient at a critical radial distance to the crack tip. The strain gradient ahead of the tip of a growing crack based on the available analytical solutions appears to be useful to examine the stress corrosion crack growth rate models based on the available experimental data.

Hutchinson [3] and Rice and Rosengren [4] presented the asymptotic stress and strain fields near a stationary crack tip in power-law hardening materials under plane strain conditions. For growing cracks, asymptotic solutions were discussed by Gao and Hwang [5] and Pan [6]. Rice, Drugan, and Sham [7] presented the asymptotic crack tip fields for a growing crack in perfectly plastic materials. For power-law hardening materials, Shoji et al. [2] presented crack growth rate models based on the analytical solutions for both stationary and growing cracks in power-law hardening materials.

The crack tip strain rate for stress corrosion crack growth can be selected at the characteristic distance in the order of the crack tip opening displacement ahead of the tip of a growing crack. Therefore, the stress and strain distributions near the tip of a stationary crack in a round compact tension specimen of elastic-plastic materials under the stress intensity factor typically considered for estimating stress corrosion crack growth rate are first obtained by finite element analyses to examine the strain gradient ahead of the crack tip. Our future work is to examine the strain gradient ahead of the tip for a growing crack.

In this paper, power-law hardening and perfectly plastic materials are considered to represent unirradiated and irradiated steels with different yield stresses and hardening behaviors. The stress-strain curves for the power-law hardening and perfectly plastic materials for the finite element analyses are selected to match those of unirradiated and irradiated stainless steels at high temperature water as presented in Chopra and Rao [8]. The computational results are obtained to examine the question that the available asymptotic stress and strain solutions are applicable for the radial distance larger than the crack tip opening displacement below which the finite strain effects must be considered. Finally, the implications of the computational results on the crack growth rate models of Shoji et al. [2] for estimation of stress corrosion crack growth rate are discussed.

CRACK TIP STRESS AND STRAIN FIELDS FOR POWER-LAW HARDENING MATERIALS

We consider an elastic power-law hardening material with the tensile stress-strain relation as

$$\begin{aligned} \varepsilon &= \frac{\sigma}{E} \quad \text{for} \quad \sigma \le \sigma_0 \\ \varepsilon &= \alpha\varepsilon_0 \left(\frac{\sigma}{\sigma_0}\right)^n \text{for} \quad \sigma > \sigma_0 \end{aligned} \tag{2}$$

where σ represents the tensile stress, ε is the tensile strain, E represents the elastic modulus, σ_0 is the initial yield stress, n represents the hardening exponent, and α is a material constant. Here, $\varepsilon_0 = \sigma_0 / E$. Since the elastic power-law hardening material is considered in this paper, the material constant α is taken as 1. We also consider an elastic perfectly plastic material with the tensile stress-strain relation as

$$\begin{aligned} \sigma &= E\varepsilon \quad \text{for} \quad \varepsilon \le \varepsilon_0 \\ \sigma &= \sigma_0 \quad \text{for} \quad \varepsilon > \varepsilon_0 \end{aligned} \tag{3}$$

Two hardening materials with the hardening exponent $n = 5$ were chosen and two perfectly plastic materials were also chosen. The values of the yield stress σ_0 are chosen to be 180 MPa and 720 MPa to represent the yield stresses of unirradiated and irradiated stainless steels at warm water temperature, respectively (Chopra and Rao [8]). The elastic modulus E is taken as 150 GPa and the Poisson's ratio ν is selected to be 0.3. The power-law hardening and perfectly plastic stress-strain relations are shown in Figure 1.

For power-law hardening materials, the near tip stresses and strains well within the plastic zone close to the crack tip can be expressed in terms of the polar coordinates r and θ centered at the crack tip as (Shih [9])

$$\sigma_{ij} = \sigma_0 \left[\frac{J}{\alpha\sigma_0\varepsilon_0 I_n r}\right]^{\frac{1}{n+1}} \tilde{\sigma}_{ij}(\theta, n) \tag{4}$$

and

$$\varepsilon_{ij} = \alpha\varepsilon_0 \left[\frac{J}{\alpha\sigma_0\varepsilon_0 I_n r}\right]^{\frac{n}{n+1}} \tilde{\varepsilon}_{ij}(\theta, n) \tag{5}$$

where σ_{ij} represent the stresses, ε_{ij} represent the strains, J represents the J integral, I_n represents the integration constant, r represents the radial distance to the tip, and $\tilde{\sigma}_{ij}$ and $\tilde{\varepsilon}_{ij}$ are dimensionless functions of the angle θ and the hardening exponent n (Shih [9]).

COMPUTATIONAL MODEL

A round compact tension specimen is considered in this investigation. Figure 2(a) shows a schematic of a round compact tension specimen. The specimen has the thickness of 8 mm. A fatigue crack with the length of 0.5 mm from the machined notch tip is considered. Therefore, the total crack length is 7.5 mm. The remaining ligament is therefore 8.5 mm based on the dimensions shown in Figure 2(a). Figures 2(b) and 2(c) show a half two-dimensional finite element model for the round compact tension specimen and a close-up view of the mesh near the crack tip, respectively. The commercial finite element program ABAQUS was employed to perform the computations. Second-order elements CPE8R with reduced integration were used for the finite element models and selected CPE8H elements with the hybrid formulation were used near the tip for better numerical stability. The total numbers of the elements for the half specimen are 1,507 for the power-law hardening materials and 1,421 for the perfectly plastic materials. The smallest element sizes in the radial direction are 17.6 nm and 57.7 nm for the power-law hardening and perfectly plastic materials, respectively. A load of 205.8 N/m is applied through a rigid bar connection to the center of the pin hole of the specimen such that the stress intensity factor K_I for the crack is 15 MPa$\sqrt{\text{m}}$ which is a typical value considered for examining stress corrosion crack growth rate.

COMPUTATIONAL RESULTS

Figures 3(a), 3(b) and 3(c) show the normalized Mises stress σ_e / σ_0, the normalized opening strain $\varepsilon_{22} / \varepsilon_0$, and the normalized effective plastic strain $\varepsilon_e^p / \varepsilon_0$ directly ahead of the tip, respectively, as functions of the radial distance to the tip in a logarithmic scale for the materials with $\sigma_0 = 180$ MPa. As shown in Figure 3(a) for the perfectly plastic material, the normalized Mises stress increases and then becomes a constant as the radial distance to the tip decreases. This is in agreement with the theoretical results. For the power-law hardening material, the normalized Mises stress increases as the radial distance decreases. The computational results for the plastic zone size R_p ahead of the crack tip are about 210 μm and 270 μm for the power-law hardening and perfectly plastic materials, respectively, which are small compared with the crack length and remaining ligament of the round compact tension specimen.

When the normalized Mises stresses are plotted in the logarithmic scale for a given range of the radial distance and the stress-distance curve becomes linear, the Mises stress can be expressed in the form of a power function of the radial distance for a given range of the radial distance. As shown in Figure 3(a) for the power-law hardening material, the slope of the normalized Mises stress continues to change as the radial distance decreases. Since the stress distribution very close to the crack tip may not be accurate, the portion of the stress curve in the range of 1 to 0.1 μm is used to determine the exponent of the power function or the singularity exponent of the crack tip stress field. The singularity exponent for the stress with respect to the radial distance is determined for this range as -0.16 which is in agreement with the HRR solution of $-1/(n+1) = -0.16$, for the power-law hardening material as listed in Equation (4). For the range of the radial distance from 1 μm to the boundary of the plastic zone, if a linear fitting curve is placed, the value of the singularity exponent will be much smaller than that of the HRR solution of $-1/(n+1) = -0.16$.

Figure 3(b) shows the normalized opening strain ε_{22} directly ahead of the tip for both the power-law hardening and perfectly plastic materials. As shown in Figure 3(b), the slope of the normalized strain continues to change as the radial distance decreases. The portion of the strain curve in the range of 1 to 0.1 μm is used to determine the exponent of the power function or the singularity exponent of the crack tip strain field. The singularity exponent for the strain with respect to the radial distance is determined for this range as -0.69 which is close to the theoretical solution of $-n/(n+1) = -0.83$, for the power-law hardening material as listed in Equation (5). For the perfectly plastic material, the slope for the strain distribution for this range is -0.22 whose value is much small than that of the theoretical solution of -1 which could occur well within the plastic zone (Shih [9]). The results for the normalized effective plastic strain $\varepsilon_e^p / \varepsilon_0$ shown in Figure 3(c) are quite similar to those shown in Figure 3(b) and will not be discussed further.

An estimation of the crack tip opening displacement δ_t for power-law hardening materials was given by Shih [9]. Under plane strain small-scale yielding conditions, the relation can be written as

$$\delta_t = d_n \frac{K_I^2 (1-\nu^2)}{E\sigma_0} \tag{6}$$

where d_n represents the coefficient which is a function of the hardening exponent n and the ratio σ_0 / E when the crack tip opening displacement is evaluated well within the HRR dominant zone (with the HRR dominant zone must be an order of magnitude larger than the crack tip opening displacement). For the power-law hardening materials, d_n for the materials with σ_0 = 180 MPa and 720 MPa are estimated as 0.28 and 0.37, respectively. For the perfectly plastic materials, d_n is 0.78. For the given value of K_I = 15 MPa$\sqrt{\mathrm{m}}$, the values of the crack tip opening displacement δ_t are estimated as 2.1 and 5.9 μm, respectively, for the power-law hardening and perfectly plastic materials with σ_0 = 180 MPa. Since the normalized Mises stress and opening strain are plotted in a logarithmic scale, the normalized Mises stress and strain at the radial distance of 2.1 μm are outside of the HRR dominant zone with the size of less than 1 μm for the power-law hardening material.

Figures 4(a), 4(b) and 4(c) show the normalized Mises stress σ_e / σ_0, the normalized opening strain $\varepsilon_{22} / \varepsilon_0$, and the normalized effective plastic strain $\varepsilon_e^p / \varepsilon_0$ directly ahead of the tip, respectively, as functions of the radial distance to the tip in a logarithmic scale for the materials with $\sigma_0 = 720$ MPa. As shown in Figure 4(a) for the perfectly plastic material, the normalized Mises stress increases and then becomes a constant as the radial distance to the tip decreases. For the power-law hardening material, the normalized Mises stress increases as the radial distance decreases. The computational results for the plastic zone size R_p ahead of the crack tip are 13 μm and 17 μm for the power-law hardening and perfectly plastic materials, respectively. The general trends shown in Figures 4(a), 4(b) and 4(c) are similar to those shown in Figures 3(a), 3(b) and 3(c). The estimations of the crack tip opening displacement δ_t for the power-law hardening and perfectly plastic materials with $\sigma_0 = 720$ MPa are 0.7 and 1.5 μm, respectively, which are closer to the plastic zone boundaries when compared to those for the materials with $\sigma_0 =$ 180 MPa. It should be mentioned that irradiated steels have much higher yield stresses.

Since the strain gradient at the critical distance to the tip can be used for correlating crack growth rate as indicated in Shoji et al. [2], the values of the strain ε_{22} and strain gradient $d\varepsilon_{22}/dr$ at the radial distance of $2\delta_t$ are listed in Table 1 for comparison. It should be noted the large deformation effects due to crack tip blunting must be accounted for in general within the radial distance of $2\delta_t$ to the tip. It also should be mentioned that the HRR dominant zones are smaller than the values of $2\delta_t$ for the power-law hardening materials that we considered in this paper. Therefore, Equation (6) may not be valid for the given stress intensity factor. However, Equation (6) may give reasonable estimations.

As listed in the table based on Equation (6), the value of the crack opening displacement δ_t for the perfectly plastic material is larger than that for the power-law hardening material for a given yield stress σ_0. However, the opening strain ε_{22} for the perfectly plastic material is smaller than that for the power-law hardening material for a given yield stress σ_0 at the radial distance of $2\delta_t$. The strain gradient shows the similar trend at the radial distance of $2\delta_t$. The strain gradient for the perfectly plastic material with the yield stress $\sigma_0 = 720$ MPa (representing an irradiated material with a high yield stress and low hardening) is about 200% of the value of the strain gradient for the power-law hardening material with the yield stress $\sigma_0 =$ 180 MPa (representing an unirradiated material with a low yield stress and high hardening) based on the computational results. The numerical results suggest that when the strain gradient or strain rate are used to correlate the stress corrosion crack growth rate based on the crack growth rate models of Andresen and Ford [1] and Shoji et al. [2], different yield stresses and hardening capabilities due to irradiation should have significant effects on the correlation.

CONCLUSIONS

In this paper, stress and strain distributions near a crack tip in a round compact tension specimen of elastic-plastic materials are obtained by finite element analyses. The strain distributions are used to explore the use of the crack tip strain distributions for crack growth rate models due to stress corrosion cracking in unirradiated and irradiated steels with different yield stresses and hardening behaviors. Both power-law hardening and perfectly plastic materials are considered. The computational results indicate that the critical radial distance to the tip based on the crack tip opening displacement is outside of the HRR dominant zone for power-law hardening materials in a round compact tension specimen under the stress intensity factor typically considered for stress corrosion cracking. For both the power-law hardening and perfectly plastic materials, the computational results show that the strain distributions are different from those of the analytical solutions for the range of the radial distance larger than the critical radial distance based on the crack opening displacement within the plastic zones. The computational results suggest that for the stress intensity factor typically considered for stress corrosion crack growth rate models, computational results are needed to estimate the strain rate for developing crack growth rate models to correlate to the experimental data.

ACKNOWLEDGEMENTS

Partial support of this work by the Michigan Memorial Phoenix Project Seed Funding Program is greatly appreciated.

REFERENCES

[1] Andresen, P. L., and Ford, F. P., 1988, "Life Prediction by Mechanistic Modeling and System Monitoring of Environmental Cracking of Iron and Nickel Alloys in Aqueous Systems," Materials Science and Engineering: A, 103(1), pp. 167-184.

[2] Shoji, T., Lu, Z., and Murakami, H., 2010, "Formulating Stress Corrosion Cracking Growth Rates by Combination of Crack Tip Mechanics and Crack Tip Oxidation Kinetics," Corrosion Science, 52(3), pp. 769-779.

[3] Hutchinson, J. W., 1968, "Singular Behaviour at the End of a Tensile Crack in a Hardening Material," Journal of the Mechanics and Physics of Solids, 16(1), pp. 13-31.

[4] Rice, J. R., and Rosengren, G. F., 1968, "Plane Strain Deformation near a Crack Tip in a Power-Law Hardening Material," Journal of the Mechanics and Physics of Solids, 16(1), pp. 1-12.

[5] Gao, Y. C. and Hwang, K. C., 1982, "Elastic-Plastic Fields in Steady Crack Growth in a Strain-Hardening Material," Proceedings of the 5th International Conference on Fracture, D. Francois, ed., Pergamon, New York, NY, pp. 669–682.

[6] Pan, H., 1988, "Investigation of Cracks Growing Steadily in Power-Law Hardening Solids," Acta Mechanica Sinica 20, pp. 142-153.

[7] Rice, J. R., Drugan, W. J., and Sham, T.-L., 1980, "Elastic-Plastic Analysis of Growing Cracks," Fracture Mechanics: Twelfth Conference. ASTM STP 700, American Society for Testing and Materials, pp. 189-221.

[8] Chopra, O. K., and Rao, A. S., 2011, "A Review of Irradiation Effects on LWR Core Internal Materials - IASCC Susceptibility and Crack Growth Rates of Austenitic Stainless Steels," Journal of Nuclear Materials, 409(3), pp. 235–256.

[9] Shih, C. F., 1981, "Relationships between the J-Integral and the Crack Opening Displacement for Stationary and Extending Cracks," Journal of the Mechanics and Physics of Solids, 29(4), pp. 305–326.

Table 1. The crack tip opening displacement δ_t, the opening strain ε_{22}, and the strain gradient $|d\varepsilon_{22}/dr|$ at the radial distance of $2\delta_t$ under the stress intensity factor of 15 $\mathrm{MPa}\sqrt{\mathrm{m}}$.

σ_0 (MPa)	n	δ_t (μm)	ε_{22} (at $r = 2\delta_t$)	$\lvert d\varepsilon_{22}/dr \rvert$ (1/mm) (at $r = 2\delta_t$)
180	5	2.1	0.00611	0.461
180	∞	5.9	0.00433	0.0688
720	5	0.7	0.0149	2.79
720	∞	1.5	0.0125	0.990

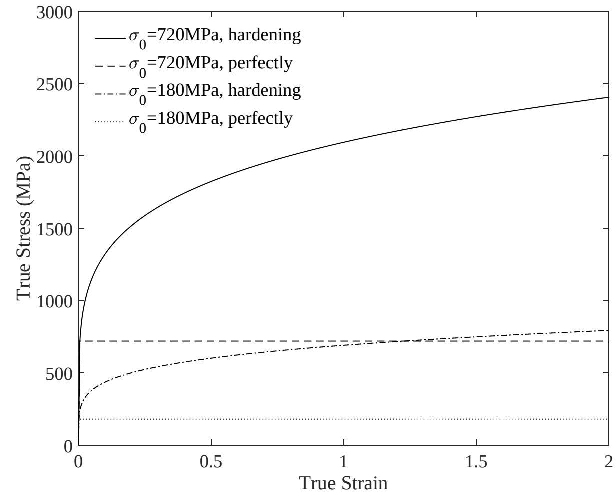

Figure 1. The elastic power-law hardening and perfectly plastic stress-strain relations considered in this investigation.

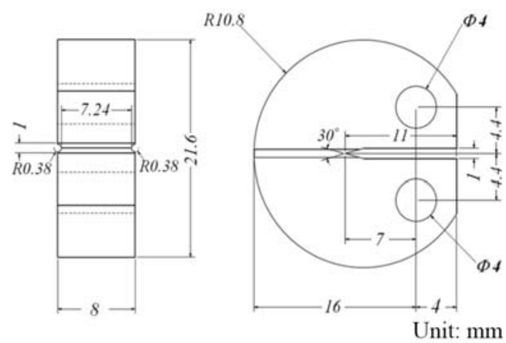

(a)

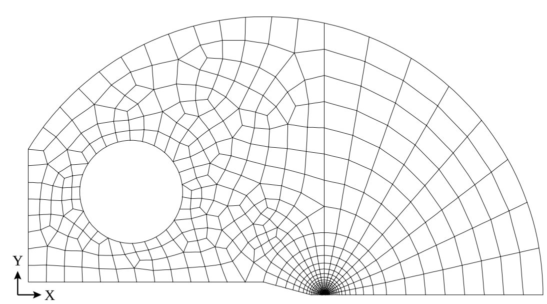

(b)

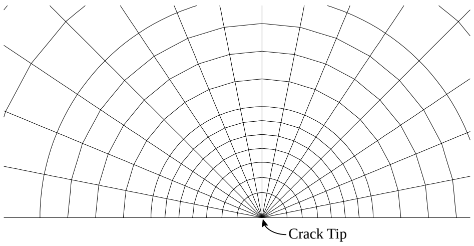

(c)

Figure 2. (a) A schematic of a round compact tension specimen with the dimensions expressed in mm, (b) a half two-dimensional finite element model for a round compact tension specimen, and (c) a close-up view of the mesh near the crack tip.

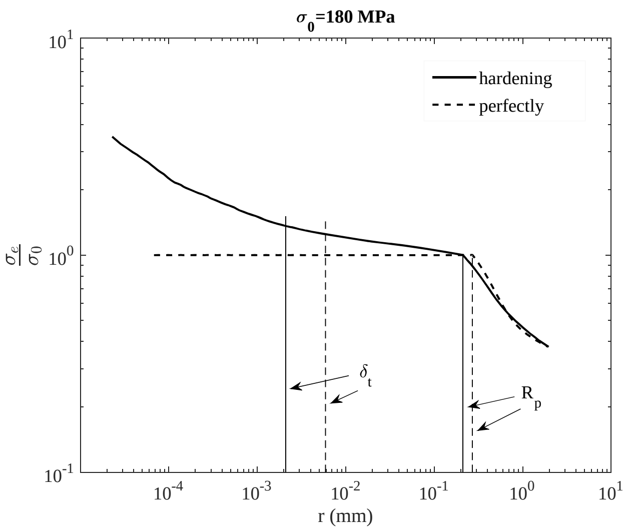

(a)

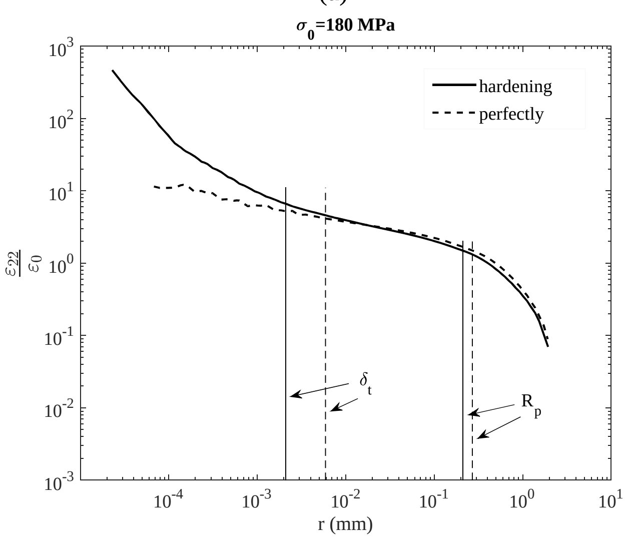

(b)

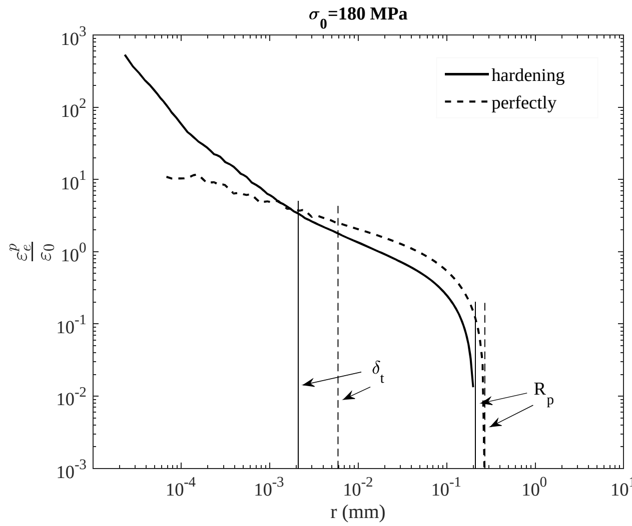

(c)

Figure 3. (a) The normalized Mises stress σ_e / σ_0 , (b) the normalized opening strain $\varepsilon_{22} / \varepsilon_0$, and (c) the normalized equivalent plastic strain $\varepsilon_e^p / \varepsilon_0$ directly ahead of the tip as functions of the radial distance to the tip for the power-law hardening and perfectly plastic materials with the yield stress $\sigma_0 =$ 180 MPa.

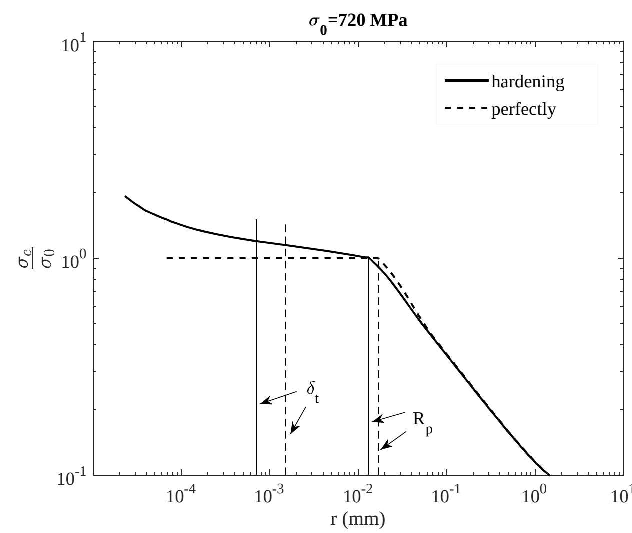

(a)

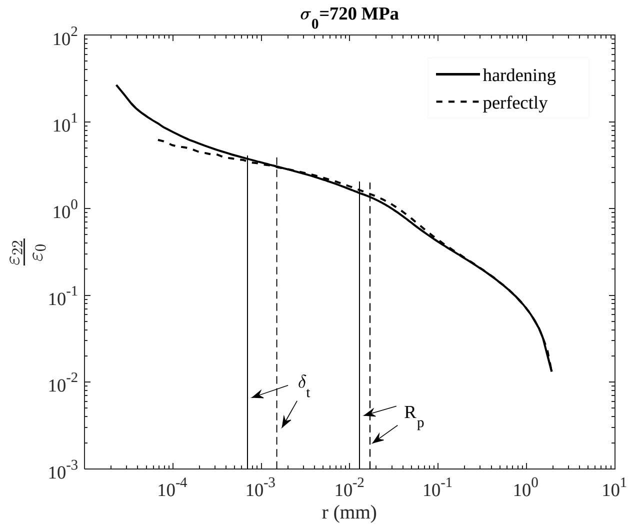

(b)

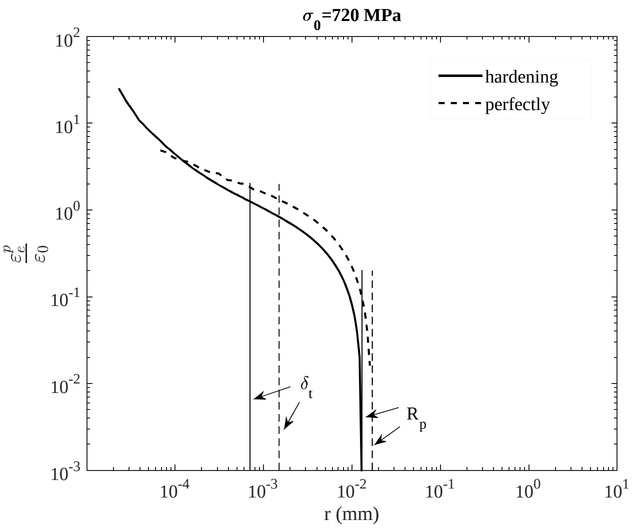

(c)

Figure 4. (a) The normalized Mises stress σ_e / σ_0, (b) the normalized opening strain $\varepsilon_{22} / \varepsilon_0$, and (c) the normalized equivalent plastic strain $\varepsilon_e^p / \varepsilon_0$ directly ahead of the tip as functions of the radial distance to the tip for the power-law hardening and perfectly plastic materials with the yield stress $\sigma_0 =$ 720 MPa.